

Supporting Information

Glycine betaine grafted nanocellulose as an effective and bio-based cationic nanocellulose flocculant for wastewater treatment and microalgal harvesting

Jonas Blockx^[1,2], An Verfaillie^[1,2], Olivier Deschaume^[3], Carmen Bartic^[3], Koenraad Muylaert*^[1], Wim Thielemans*^[2]

[1] Sustainable Materials laboratory, Department of Chemical Engineering, KU Leuven, Campus Kulak Kortrijk, Etienne Sabbelaan 53 box 7659, 8500 Kortrijk, Belgium. E-mail: wim.thielemans@kuleuven.be

[2] Laboratory for Aquatic Biology, KU Leuven, Campus Kulak Kortrijk, Etienne Sabbelaan 53 box 7659, 8500 Kortrijk, Belgium. E-mail: koenraad.muylaert@kuleuven.be

[3] Soft Matter and Biophysics Unit, Department of Physics and Astronomy, KU Leuven, Celestijnenlaan 200 D, 3001 Leuven, Belgium.

Number of pages: 25

Number of figures: 23

Number of tables: 9

Table of Contents

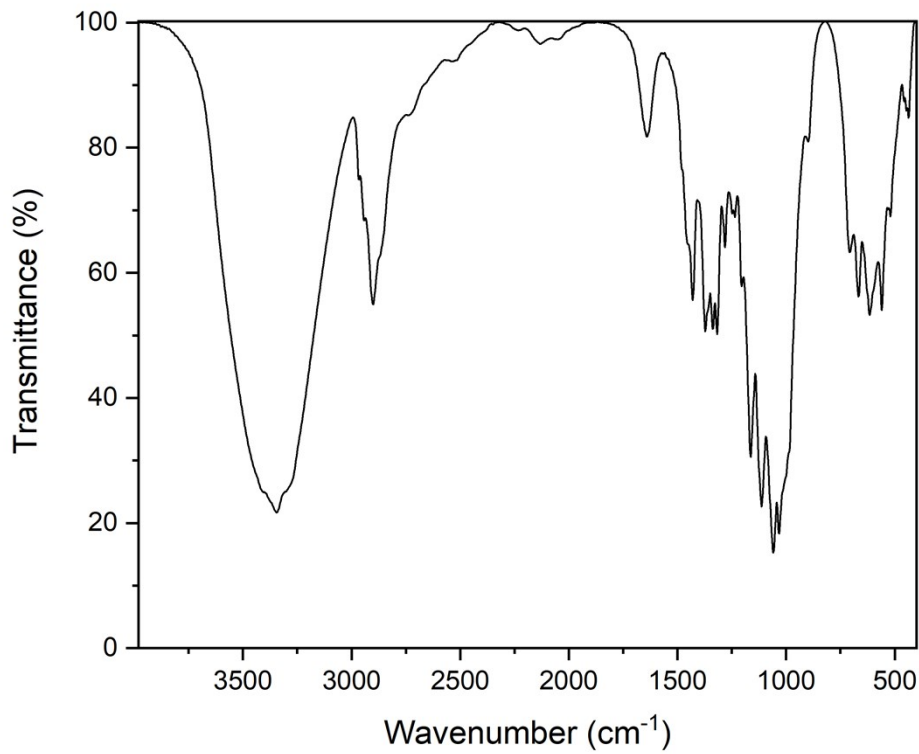
S1 FTIR data	3
S2 ζ -Potential	5
S3 Measured values EA and TGA and calculated DS values	6
S4 XPS tables	7
S5 XPS figures	12
Wide scans.....	12
Carbon 1s spectra	14
Oxygen 1s spectra	15
Nitrogen 1s spectra	16
Chlorine 2p spectra	17
S6 AFM figures and distributions	18
S7 Sigmoidal models for dose – response flocculation curves	24
S8 Flocculation of kaolin at different pH values.	25

S1 FTIR data

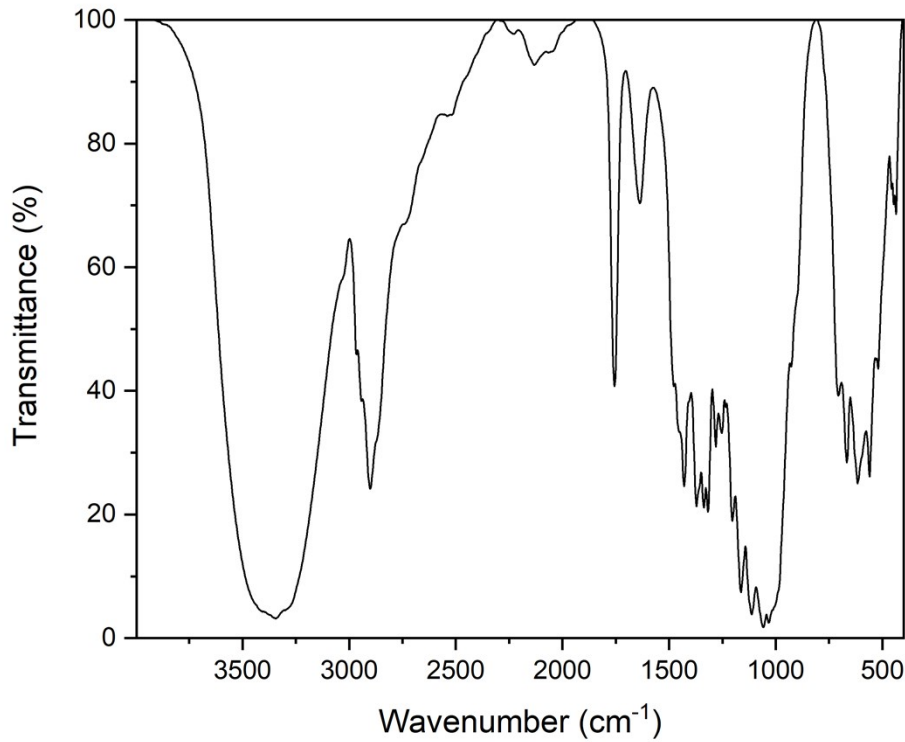
Results for the Fourier Transform Infrared spectroscopy are presented below for the unmodified CNCs and the CNCs modified with glycine betaine with a DS = 0.152 ± 0.002 . All other modifications show a similar graph and peaks as the presented modification.

bond (unmod. CNC)	wave number cm ⁻¹ unmod. CNC	wave number cm ⁻¹ BET DS = 0.152 ± 0.002
v (O-H)	3344.16	3344.75
v (C-H)	2902.93	2900.14
v (C=O)		1755.99
δ (H ₂ O) / v (C=C)/ v (C=N)	1640.02	1637.70
δ (C-O-H)	1432.20	1429.68
δ (C-O-H)	1372.03	1372.57
δ (C-O-H)	1321.84	1317.51
v (C-O, ester)		1280.79
v (C-O-C, glycosidic, asym.)	1166.41	1162.50
v (C-OH)	1117.05	1111.52
v (C-OH)	1064.65	1058.49
ω (C-OH)		705.66
ω (C-OH)	668.78	666.91
ω (C-OH)	617.27	615.92
ω (C-OH)	558.54	558.82

SI Table 1: Data table FTIR peaks for the unmodified CNCs¹ and the bet-g-CNCs with a DS = 0.152 ± 0.002 .



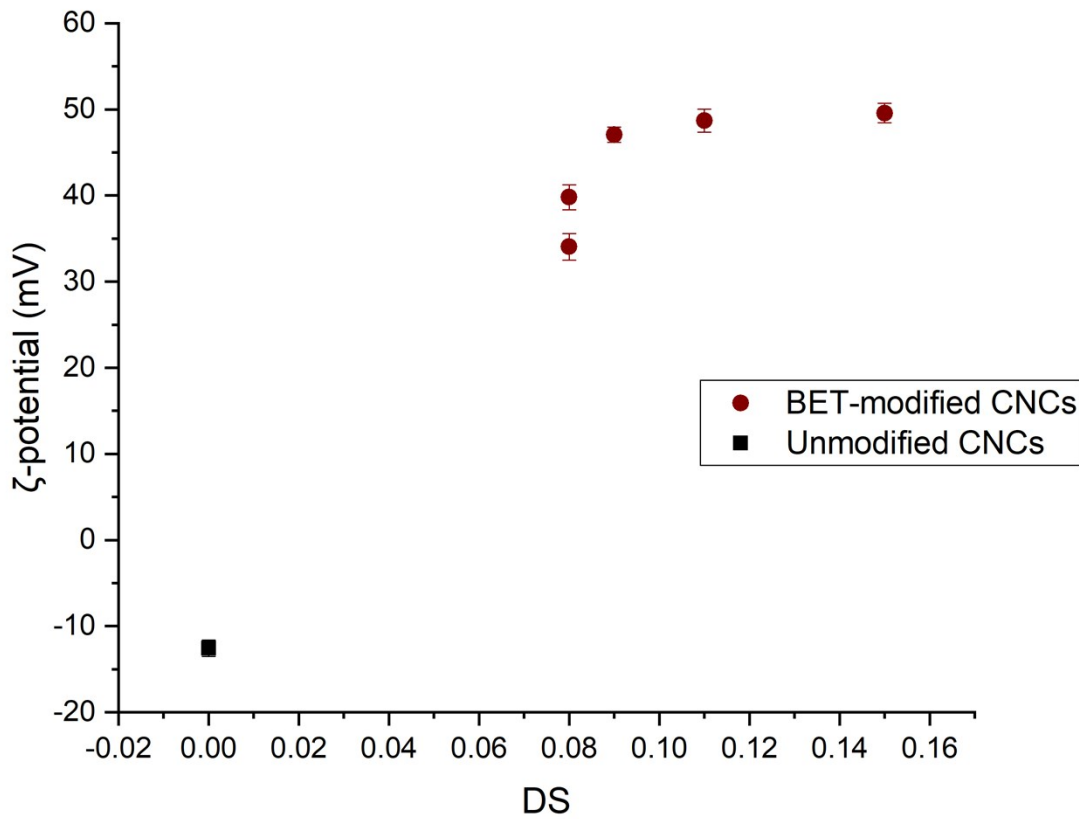
SI Figure 1: FTIR graph unmodified CNCs¹



SI Figure 2: FTIR graph bet-g-CNCs with $DS = 0.152 \pm 0.002$

S2 ζ -Potential

ζ -potential measurements were performed to assess the presence of cationic charges in the samples after modification. The unmodified CNCs had a slightly negative ζ -potential (-12.55 ± 0.95 mV), while all the modifications had a clear positive potential (between 34.04 ± 1.56 and 49.57 ± 1.15 mV). In general the ζ -potential increases with increasing DS.



SI Figure 3: ζ -potential of the unmodified and bet-g-CNCs.

S3 Measured values EA and TGA and calculated DS values

SI Table 2: EA and TGA results as well as calculated elemental results and empirical formula.

		Unmodified	DS = 0.152 ± 0.002	DS = 0.107 ± 0.002	DS = 0.091 ± 0.004	DS = 0.080 ± 0.003	DS = 0.078 ± 0.003
Found	C	44.54	43.81	43.9	43.78	43.04	43.82
	H	6.23	6.41	6.31	6.34	6.34	6.28
	N	0.19	1.14	0.83	0.72	0.63	0.62
Wt% absorbed water		4.49	2.39	2.02	1.82	2.24	1.91
Calculated formula		C ₆ H ₁₀ O ₅	C _{6.75} H _{11.50} O _{5.15} N _{0.15} Cl _{0.15}	C _{6.53} H _{11.07} O _{5.11} N _{0.11} Cl _{0.11}	C _{6.46} H _{10.91} O _{5.09} N _{0.09} Cl _{0.09}	C _{6.39} H _{10.80} O _{5.08} N _{0.08} Cl _{0.08}	C _{6.39} H _{10.78} O _{5.08} N _{0.08} Cl _{0.08}
Calculated	C	42.45	43.37	43.53	43.61	43.44	43.59
	H	6.44	6.47	6.42	6.39	6.4	6.39
	N	0.00	1.13	0.93	0.72	0.63	0.62
	O	51.11	46.19	47.13	47.45	47.93	47.84
	Cl	0.00	1.57	2.10	1.82	1.60	1.57

S4 XPS tables

SI Table 3: XPS data for the unmodified CNCs.¹

<i>Orbital</i>	<i>Component</i>	<i>Binding energy / eV</i>	<i>FWHM / eV</i>	<i>rel. A /%</i>	<i>At %</i>
<i>C 1s</i>	C-C	285.00	1.09	3.06	5.13
	C-O	286.82	1.09	80.90	135.69
	O-C-O	288.33	1.09	17.04	28.58
	All			100.00	59.62
<i>O 1s</i>	C-O-H	532.99	1.17	59.88	24.11
	O-C-O	533.59	1.17	40.12	16.16
	All			100.00	40.27
<i>Zn 2p</i>	Zn	1015.02	1.45		
	All			100.00	0.11

SI Table 4: XPS data for bet-g-CNCs with DS = 0.152 ± 0.002.

<i>Orbital</i>	<i>Component</i>	<i>Binding energy / eV</i>	<i>FWHM / eV</i>	<i>rel. A /%</i>	<i>At %</i>
<i>C 1s</i>	C-C/C=C	285.11	1.19	3.43	2.20
	C-O/C-N	286.76	1.19	71.44	45.73
	O-C-O	288.00	1.19	17.56	11.24
	O-C=O	289.98	1.19	7.58	4.85
	All			100.01	64.01
<i>O 1s</i>	C=O	532.29	1.56	0.61	0.18
	C-O-H	532.89	1.56	59.15	17.38
	O-C-O	533.19	1.56	39.64	11.65
	O*-C=O	533.69	1.56	0.61	0.18
	All			100.01	29.38
<i>N 1s</i>	N	403.20	1.23		
	All			100.00	3.49
<i>Cl 2p</i>	Cl- j= 1/2	197.56	1.05	66.67	2.09
	Cl- j= 3/2	199.16	1.05	33.33	1.04
	All			100.00	3.13

SI Table 5: XPS data for bet-g-CNCs with DS = 0.107 ± 0.004 .

<i>Orbital</i>	<i>Component</i>	<i>Binding energy / eV</i>	<i>FWHM / eV</i>	<i>rel. A /%</i>	<i>At %</i>
<i>C 1s</i>	C-C/C=C	285.11	1.13	3.78	2.35
	C-O/C-N	286.73	1.13	72.09	44.87
	O-C-O	288.07	1.13	19.25	11.98
	O-C=O	289.97	1.13	4.88	3.04
	All			100.00	62.25
<i>O 1s</i>	C=O	532.22	1.43	0.98	0.33
	C-O-H	532.62	1.43	58.70	19.92
	O-C-O	533.12	1.43	39.34	13.35
	O*-C=O	533.82	1.43	0.98	0.33
	All			100.00	33.94
<i>N 1s</i>	N	403.27	1.34		
	All			100.00	2.01
<i>Cl 2p</i>	Cl- j= 1/2	197.72	1.12	63.31	1.14
	Cl- j= 3/2	199.32	1.12	31.65	0.57
	Cl-C j= 1/2	200.59	1.12	3.36	0.06
	Cl-C j= 3/2	202.19	1.12	1.68	0.03
	All			100.00	1.80

SI Table 6: XPS data for bet-g-CNCs with DS = 0.091 ± 0.004.

<i>Orbital</i>	<i>Component</i>	<i>Binding energy / eV</i>	<i>FWHM / eV</i>	<i>rel. A /%</i>	<i>At %</i>
<i>C 1s</i>	C-C/C=C	285.04	1.13	2.22	1.39
	C-O/C-N	286.72	1.13	73.36	45.78
	O-C-O	288.06	1.13	17.86	11.14
	O-C=O	289.93	1.13	4.56	2.85
	All			100.00	62.41
<i>O 1s</i>	C=O	532.21	1.39	1.28	0.43
	C-O-H	532.81	1.39	58.35	19.55
	O-C-O	533.11	1.39	39.10	13.10
	O*-C=O	533.61	1.39	1.28	0.43
	All			100.01	33.51
<i>N 1s</i>	N	403.22	1.31		
	All			100.00	1.98
<i>Cl 2p</i>	Cl- j= 1/2	197.68	1.11	63.20	1.33
	Cl- j= 3/2	199.28	1.11	31.59	0.67
	Cl-C j= 1/2	200.37	1.11	3.47	0.07
	Cl-C j= 3/2	201.97	1.11	1.71	0.04
	All			99.97	2.11

SI Table 7: XPS data for bet-g-CNCs with DS = 0.080 ± 0.003.

<i>Orbital</i>	<i>Component</i>	<i>Binding energy / eV</i>	<i>FWHM / eV</i>	<i>rel. A /%</i>	<i>At %</i>
<i>C 1s</i>	C-C/C=C	285.11	1.12	2.68	1.65
	C-O/C-N	286.73	1.12	75.50	46.61
	O-C-O	288.13	1.12	18.64	11.50
	O-C=O	289.93	1.12	3.37	2.08
	All			99.99	61.74
<i>O 1s</i>	C=O	532.15	1.38	0.70	0.25
	C-O-H	532.85	1.38	59.03	21.00
	O-C-O	533.15	1.38	39.56	14.07
	O*-C=O	533.65	1.38	0.70	0.25
	All			99.99	35.57
<i>N 1s</i>	N	403.31	1.41		
	All			100.00	1.30
<i>Cl 2p</i>	Cl- j= 1/2	197.80	1.15	60.52	0.84
	Cl- j= 3/2	199.40	1.15	30.25	0.42
	Cl-C j= 1/2	200.59	1.15	6.15	0.09
	Cl-C j= 3/2	201.19	1.15	3.07	0.04
	All			99.97	1.39

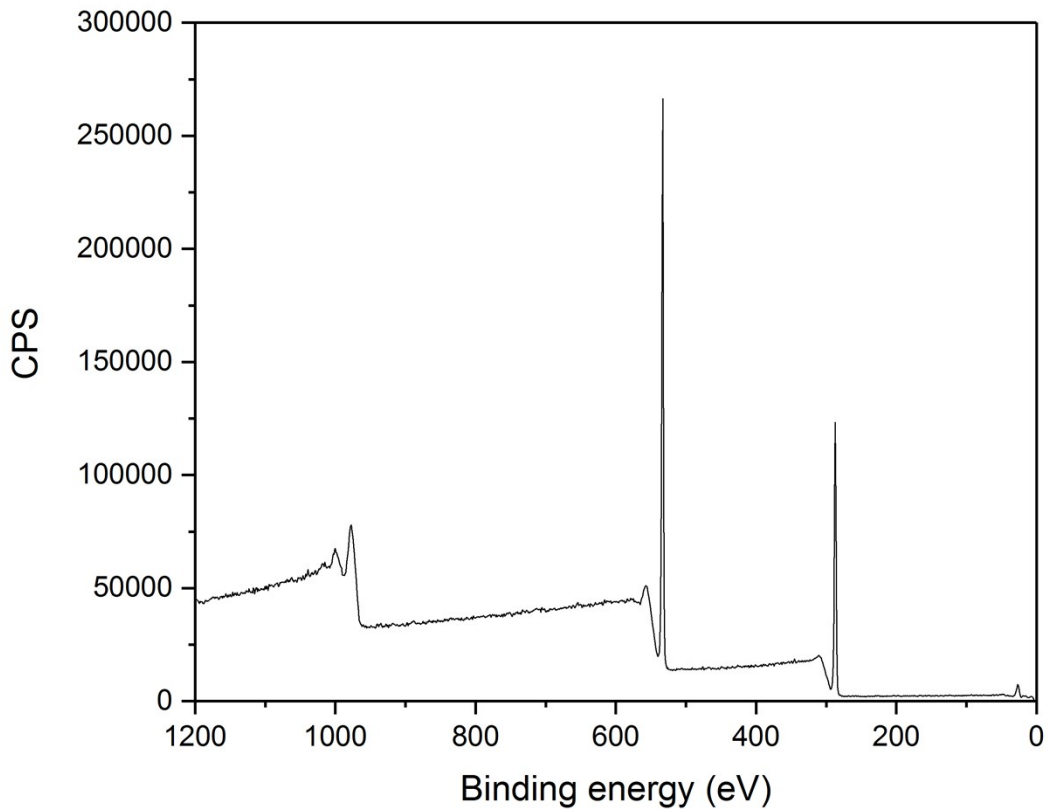
<i>Orbital</i>	<i>Component</i>	<i>Binding energy / eV</i>	<i>FWHM / eV</i>	<i>rel. A /%</i>	<i>At %</i>
<i>C 1s</i>	C-C/C=C	285.00	1.14	2.38	1.44
	C-O/C-N	286.74	1.14	76.09	46.18
	O-C-O	288.14	1.14	18.49	11.22
	O-C=O	289.86	1.14	3.04	1.84
	All			100.00	60.69
<i>O 1s</i>	C=O	532.25	1.38	0.77	0.28
	C-O-H	532.85	1.38	58.95	21.75
	O-C-O	533.15	1.38	39.51	14.58
	O*-C=O	533.65	1.38	0.77	0.28
	All			99.99	36.89
<i>N 1s</i>	N	403.19	1.40		
	All			100.00	1.22
<i>Cl 2p</i>	Cl- j= 1/2	197.79	1.19	61.17	0.73
	Cl- j= 3/2	199.39	1.19	30.58	0.36
	Cl-C j= 1/2	200.56	1.19	5.50	0.07
	Cl-C j= 3/2	202.16	1.19	2.75	0.03
	All			99.97	1.19

SI Table 8: XPS data for bet-g-CNCs with DS = 0.078 ± 0.003.

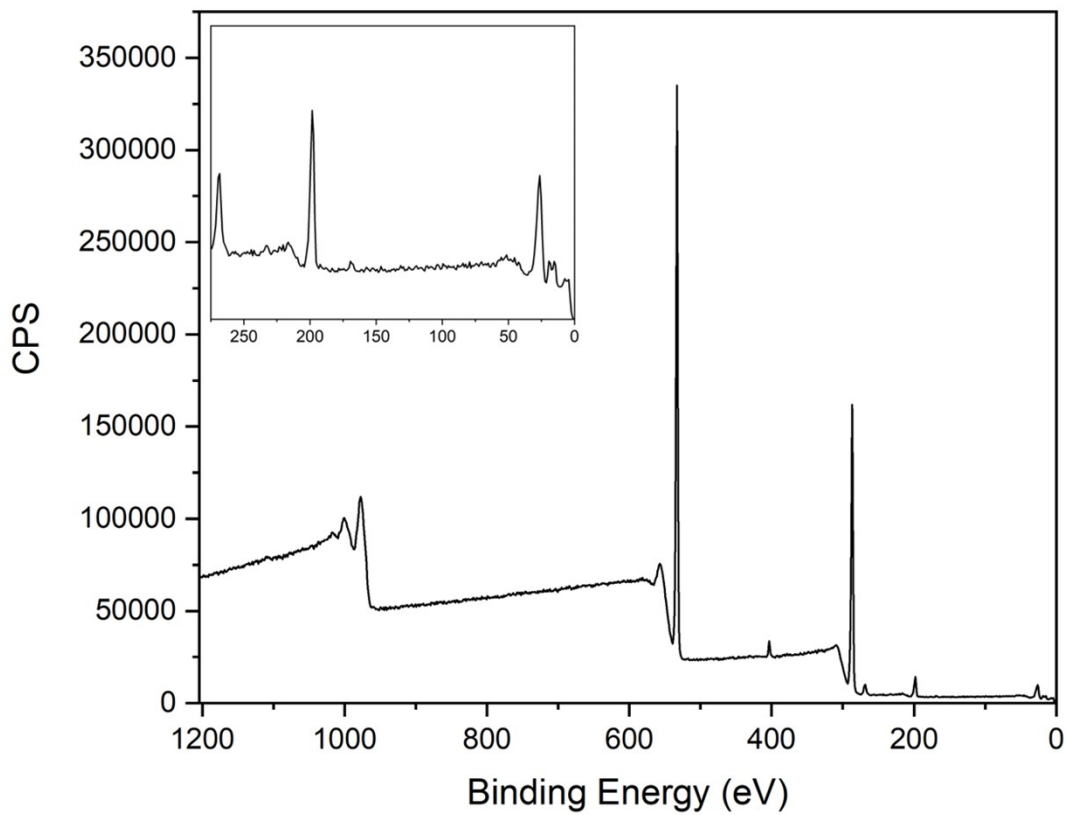
S5 XPS figures

Wide scans

XPS wide scans were taken of the unmodified and all unmodified CNCs. The results of the unmodified CNCs were published before in Blockx et al. 2019 and are also shown below.¹ As an example the wide scan of the bet-g-CNCs with $DS = 0.080 \pm 0.003$. All other modifications have a similar scan.



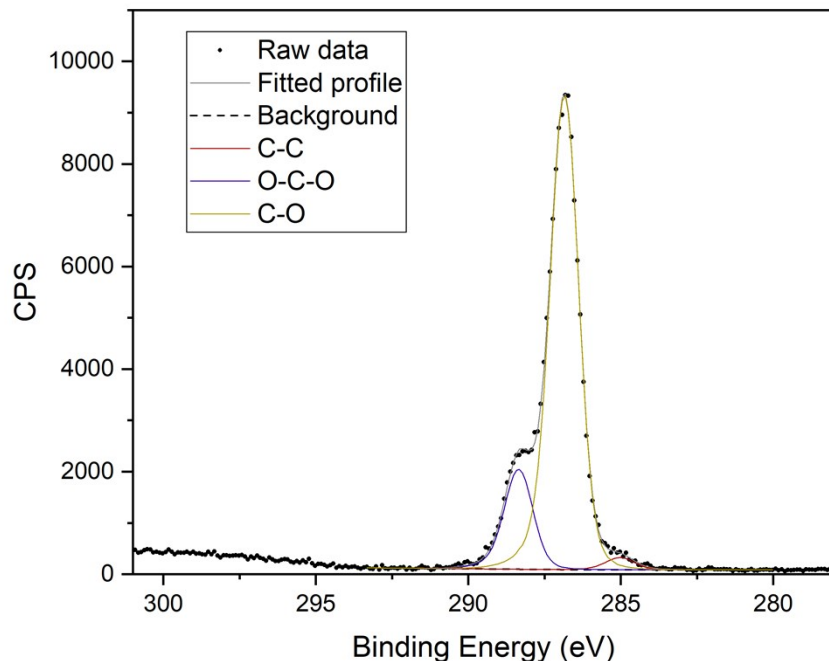
SI Figure 4: Wide XPS scan of unmodified CNCs.¹



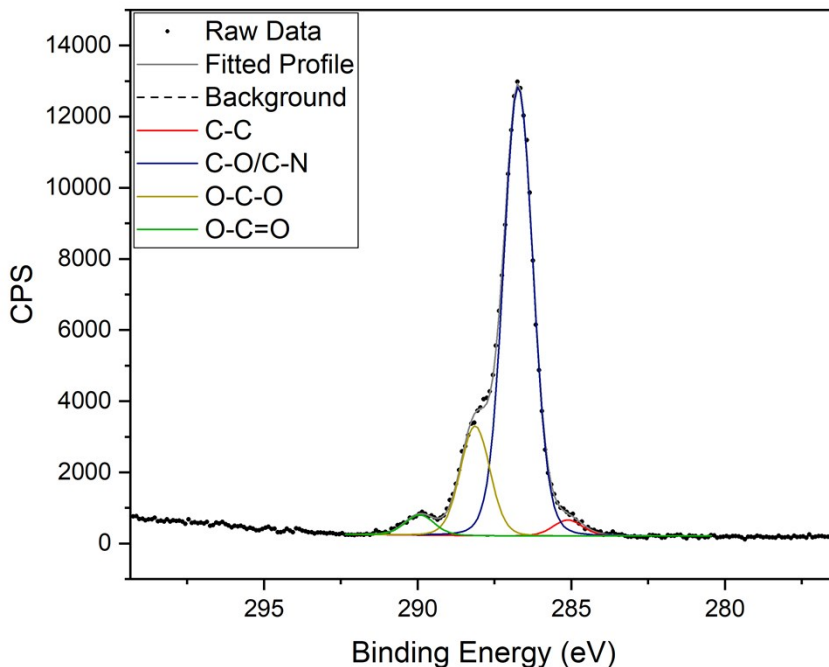
SI Figure 5: Wide XPS scan of bet-g-CNCs with DS = 0.080 ± 0.003 .

Carbon 1s spectra

The carbon 1s spectra are shown of the unmodified CNCs (published earlier by Blockx et al. 2019¹) and the bet-g-CNCs with DS = 0.080 ± 0.003 . The other modifications have a similar spectrum.



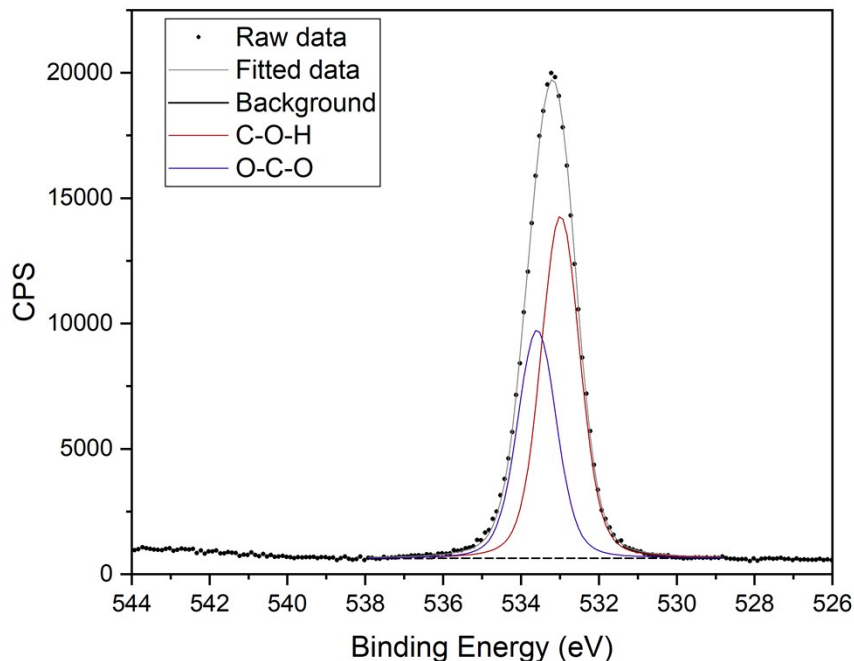
SI Figure 6: C1s spectrum of unmodified CNCs.¹



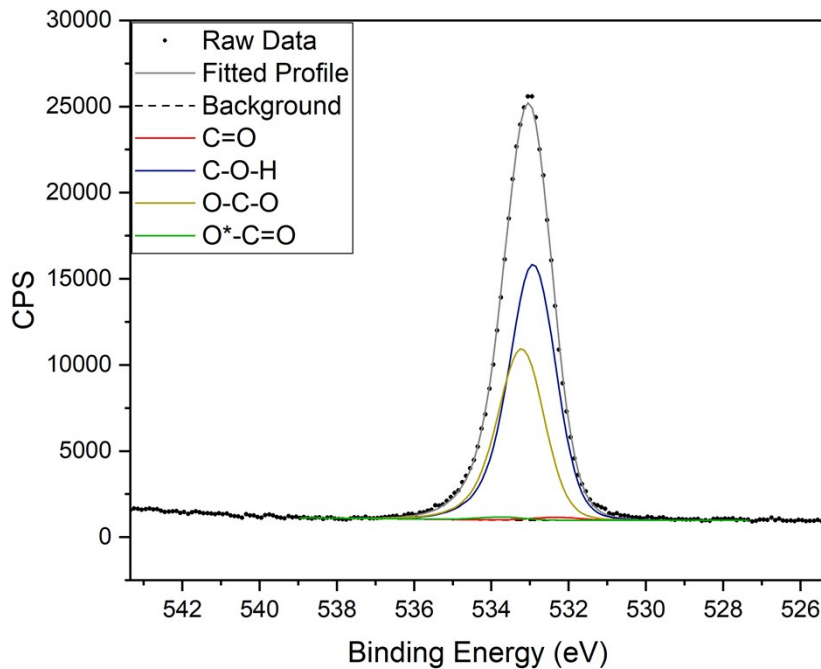
SI Figure 7: C1s spectrum of bet-g-CNCs with DS = 0.080 ± 0.003 .

Oxygen 1s spectra

The oxygen 1s spectra are shown of the unmodified CNCs (published earlier by Blockx et al. 2019¹) and the bet-g-CNCs with DS = 0.080 ± 0.003 . The other modifications have a similar spectrum.



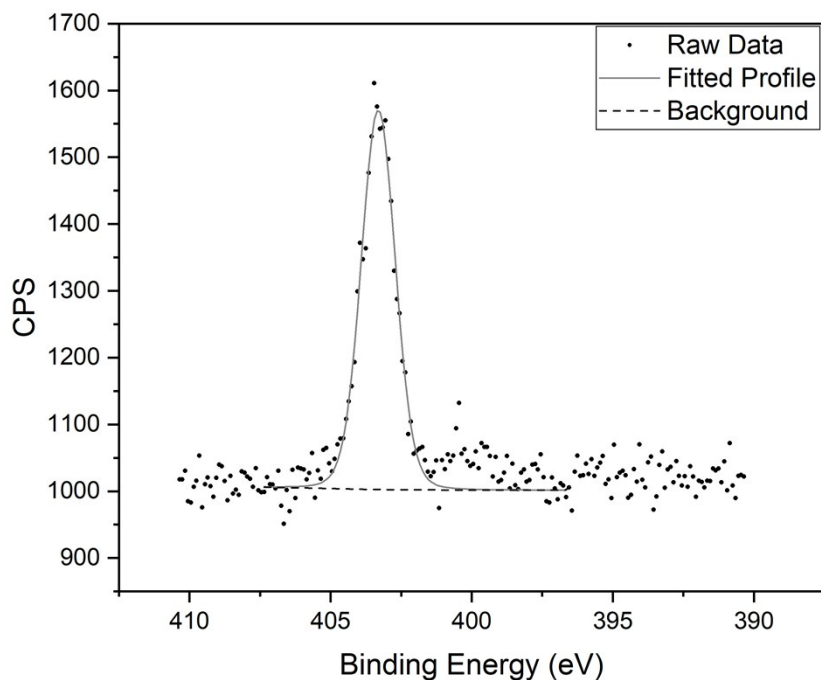
SI Figure 8: O1s spectrum of unmodified CNCs.¹



SI Figure 9: O1s spectrum of bet-g-CNCs with DS = 0.080 ± 0.003 .

Nitrogen 1s spectra

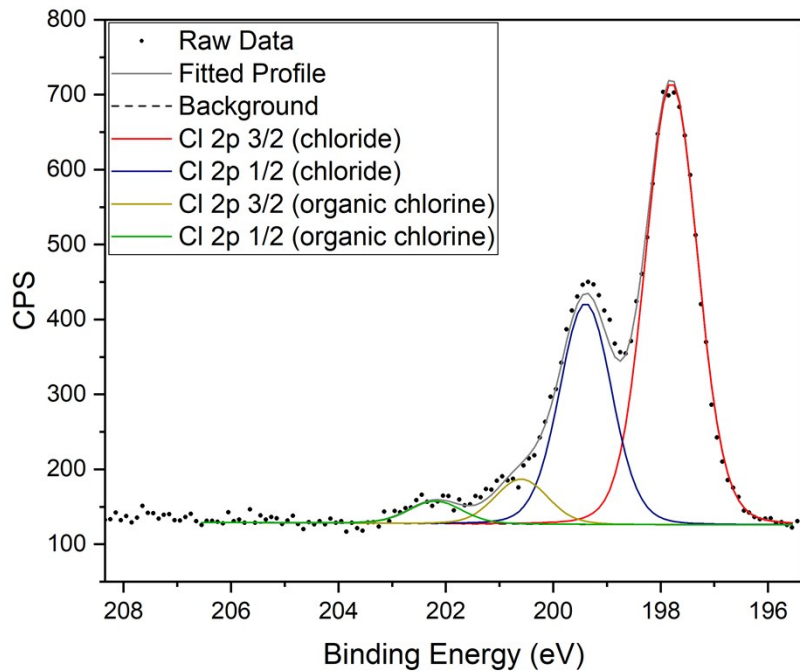
The nitrogen 1s spectrum of the bet-g-CNCs with a $DS = 0.080 \pm 0.003$ is shown below. All the other modifications have similar spectra.



SI Figure 10: N1s spectrum of bet-g-CNCs with $DS = 0.08 \pm 0.003$.

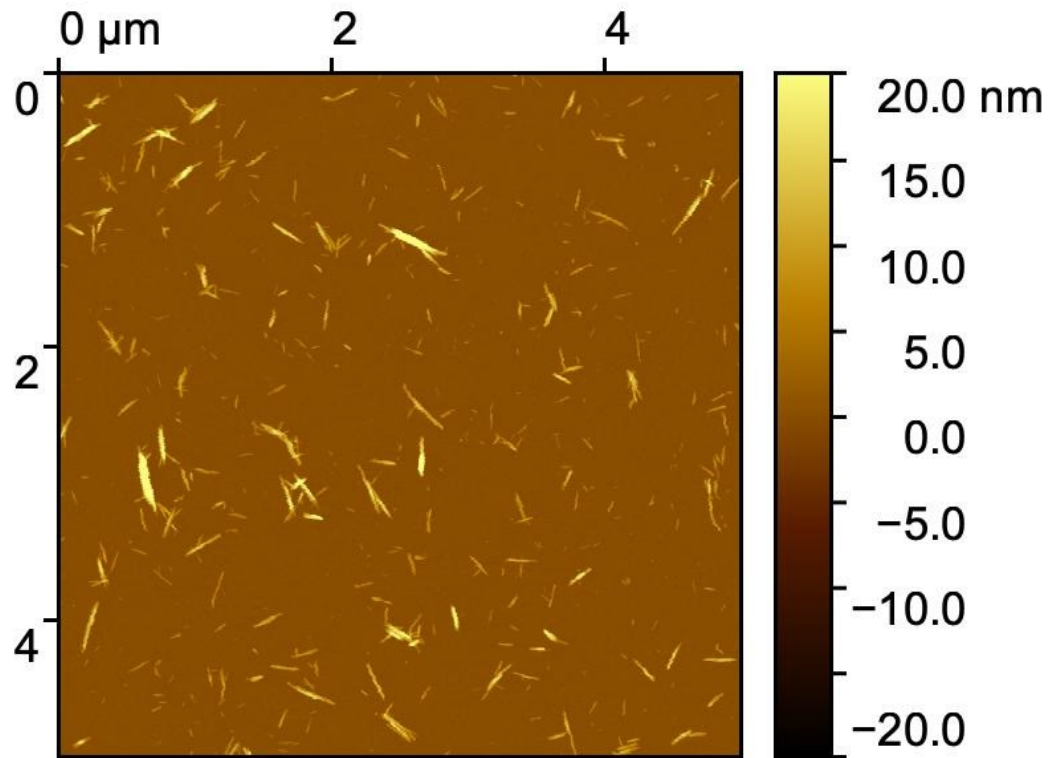
Chlorine 2p spectra

The chlorine 2p spectrum of the bet-g-CNCs with a $DS = 0.080 \pm 0.003$ is shown below. All the other modifications have similar spectra, except for the bet-g-CNCs with $DS = 0.152 \pm 0.002$, which did not show the two organic chlorine peaks.

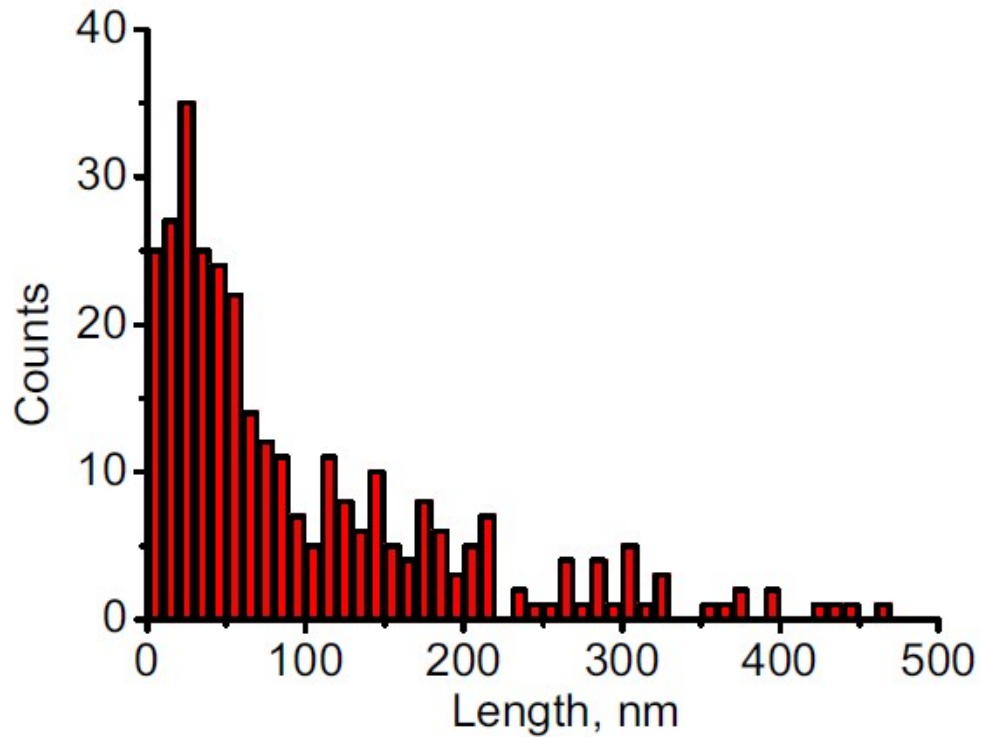


SI Figure 11: Cl₂p spectrum of bet-g-CNCs with $DS = 0.080 \pm 0.003$.

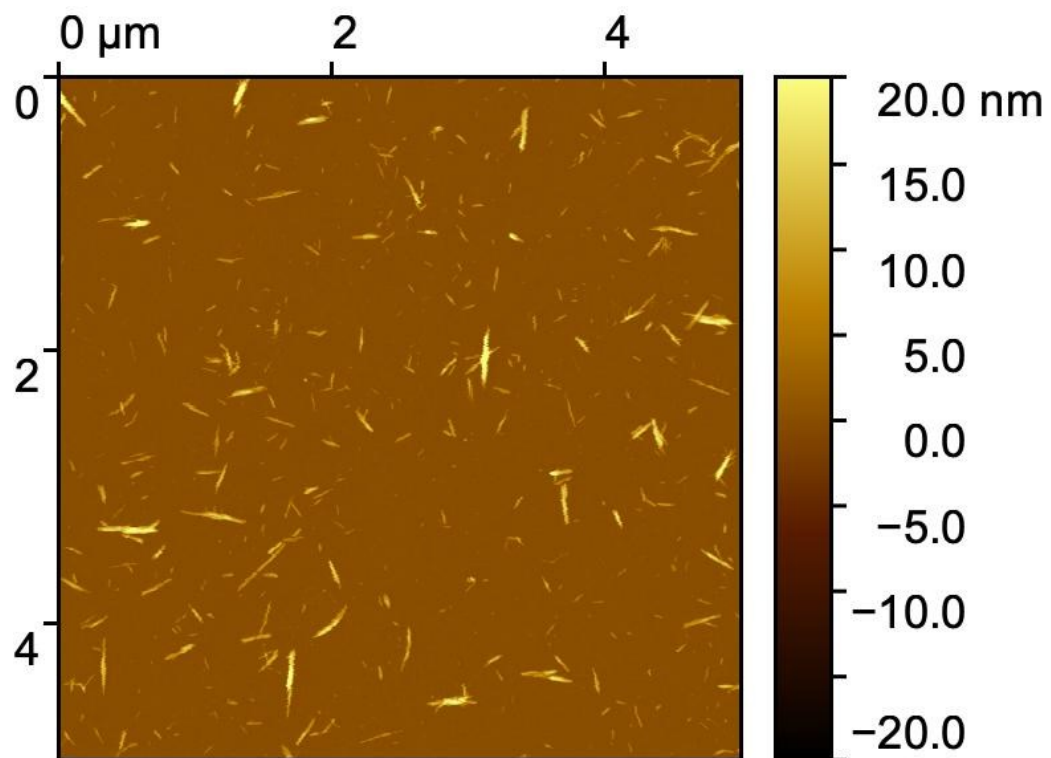
S6 AFM figures and distributions



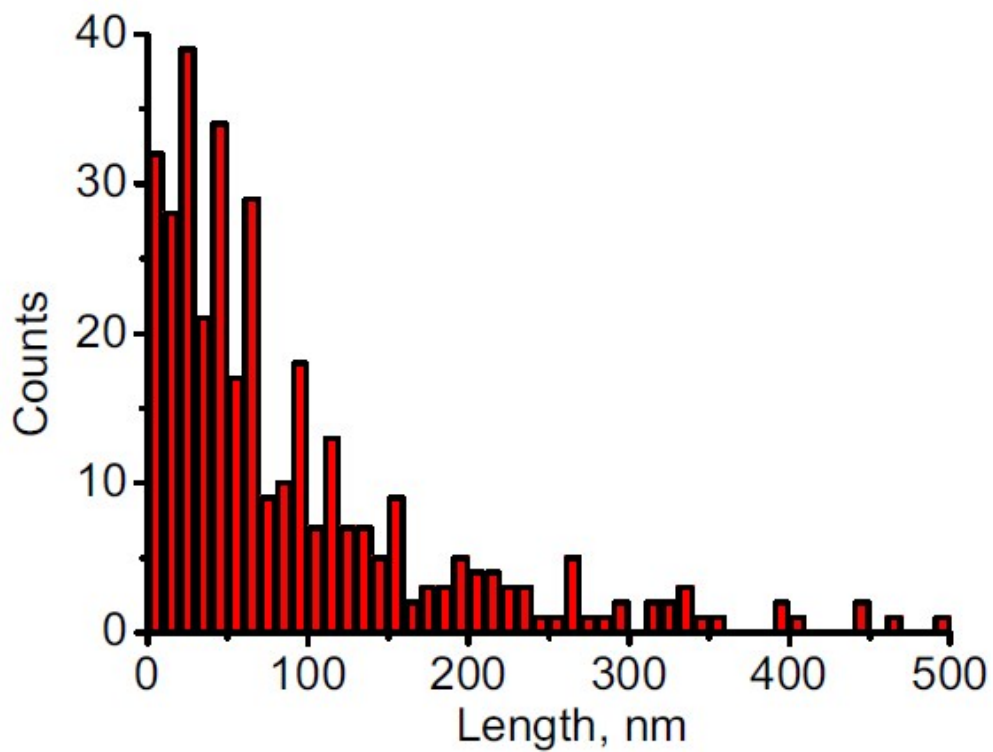
SI Figure 12: AFM image of bet-g-CNCs with $DS = 0.152 \pm 0.002$



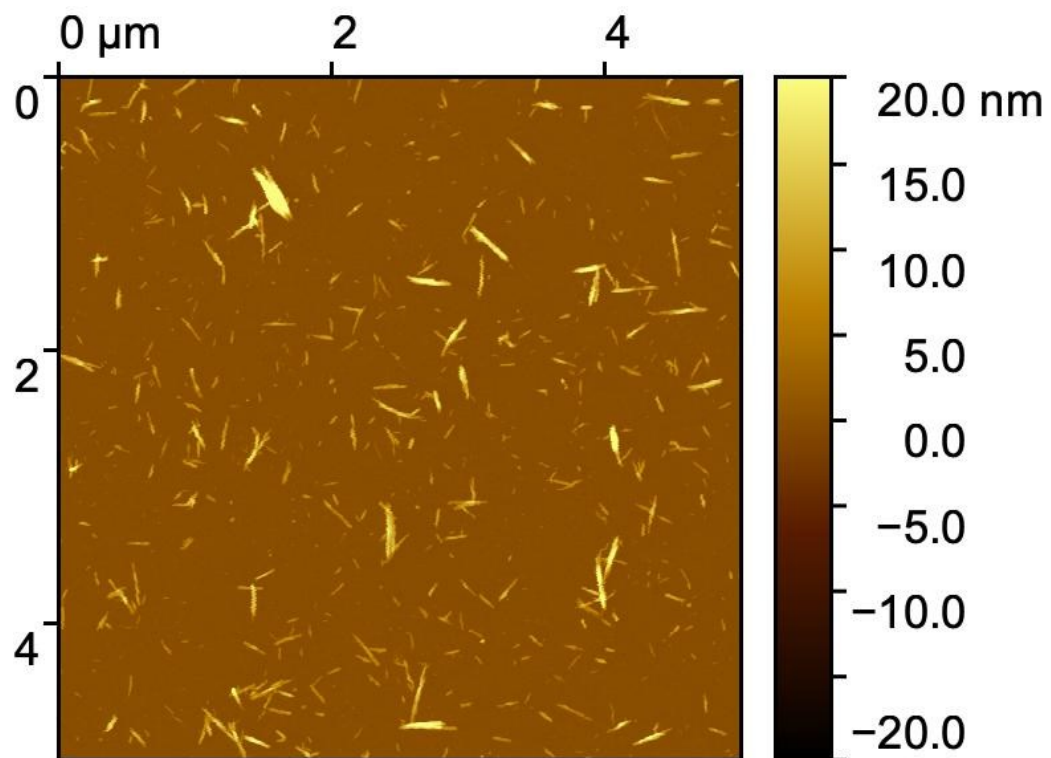
SI Figure 13: Size distribution measured with AFM of bet-g-CNCs with $DS = 0.152 \pm 0.002$ with an average size of 100 ± 110 nm.



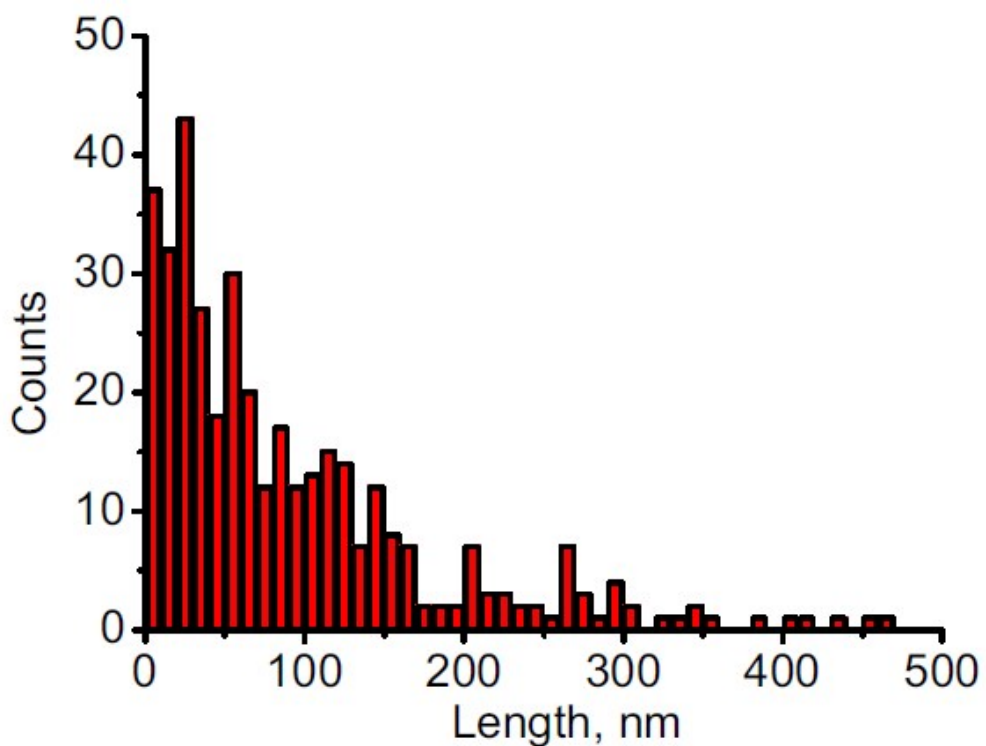
SI Figure 14: AFM image of bet-g-CNCs with $DS = 0.107 \pm 0.002$



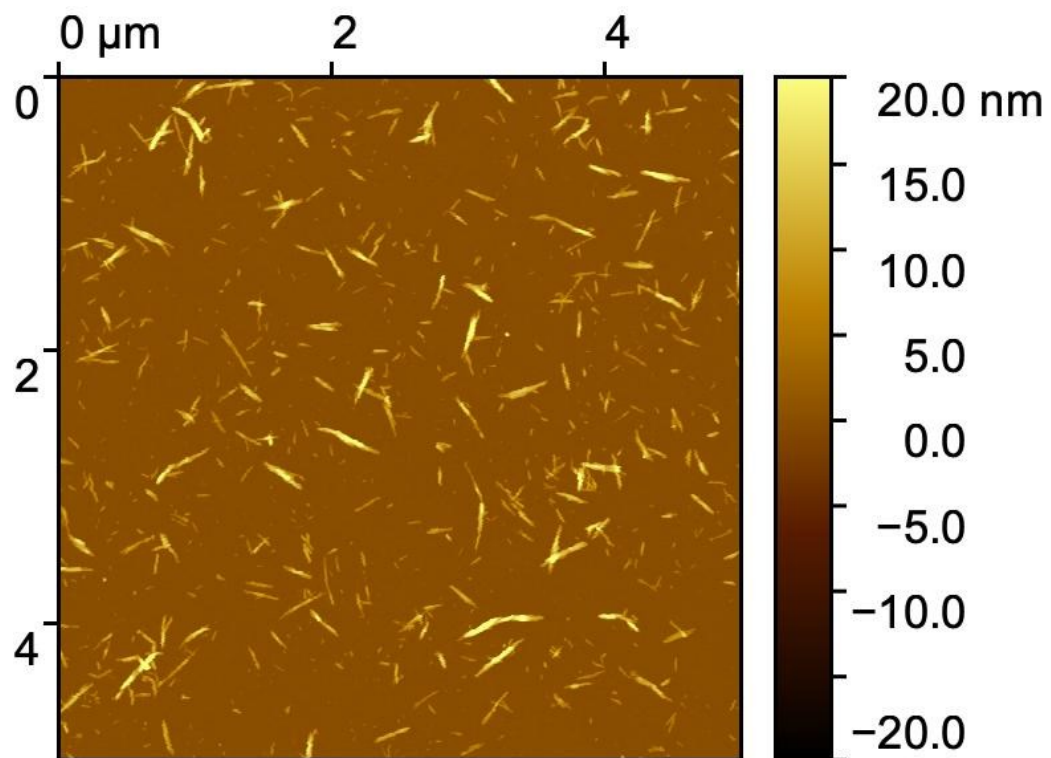
SI Figure 15: Size distribution measured with AFM of bet-g-CNCs with $DS = 0.107 \pm 0.002$ with an average size of 86 ± 97 nm.



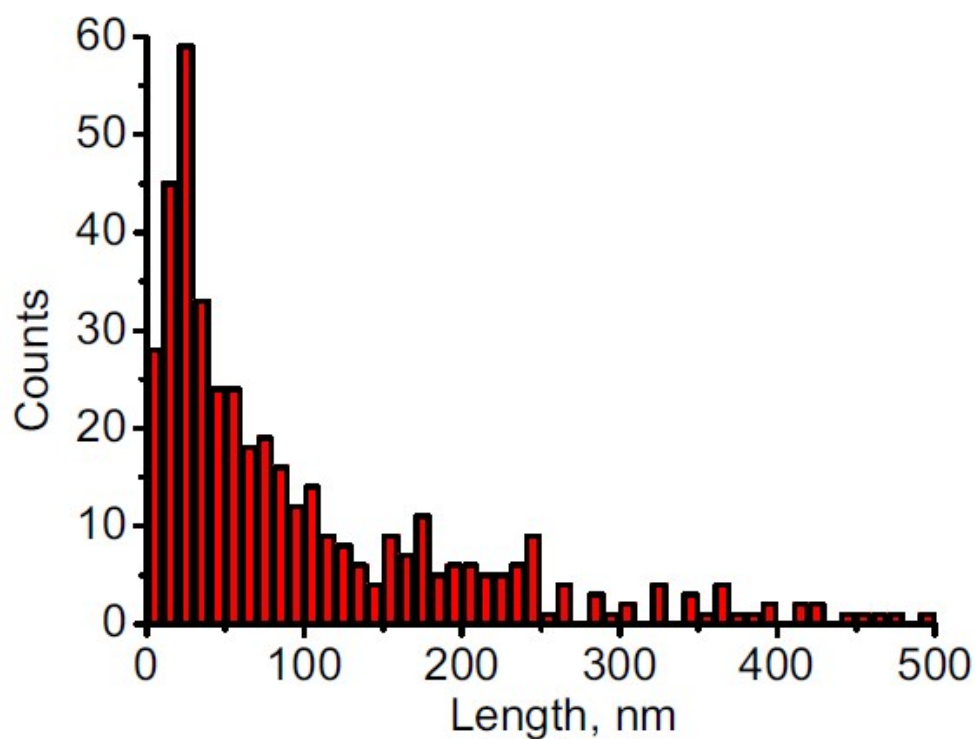
SI Figure 16: AFM image of bet-g-CNCs with $DS = 0.091 \pm 0.004$



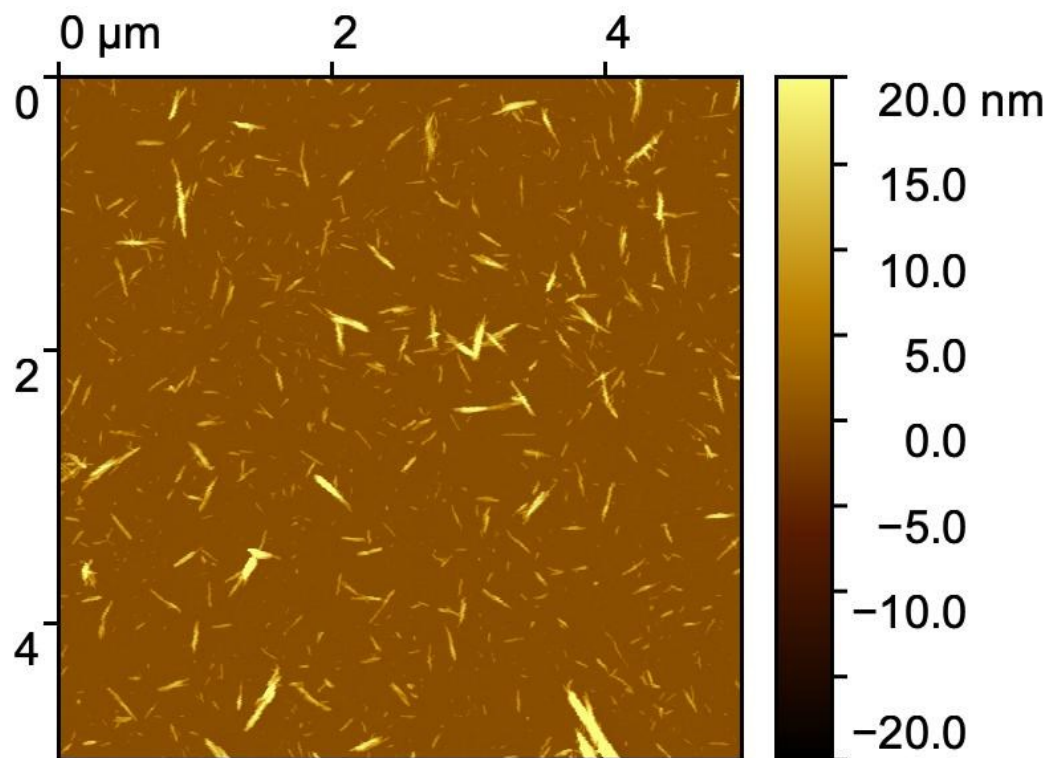
SI Figure 17: Size distribution measured with AFM of bet-g-CNCs with $DS = 0.091 \pm 0.004$ with an average size of 91 ± 104 nm.



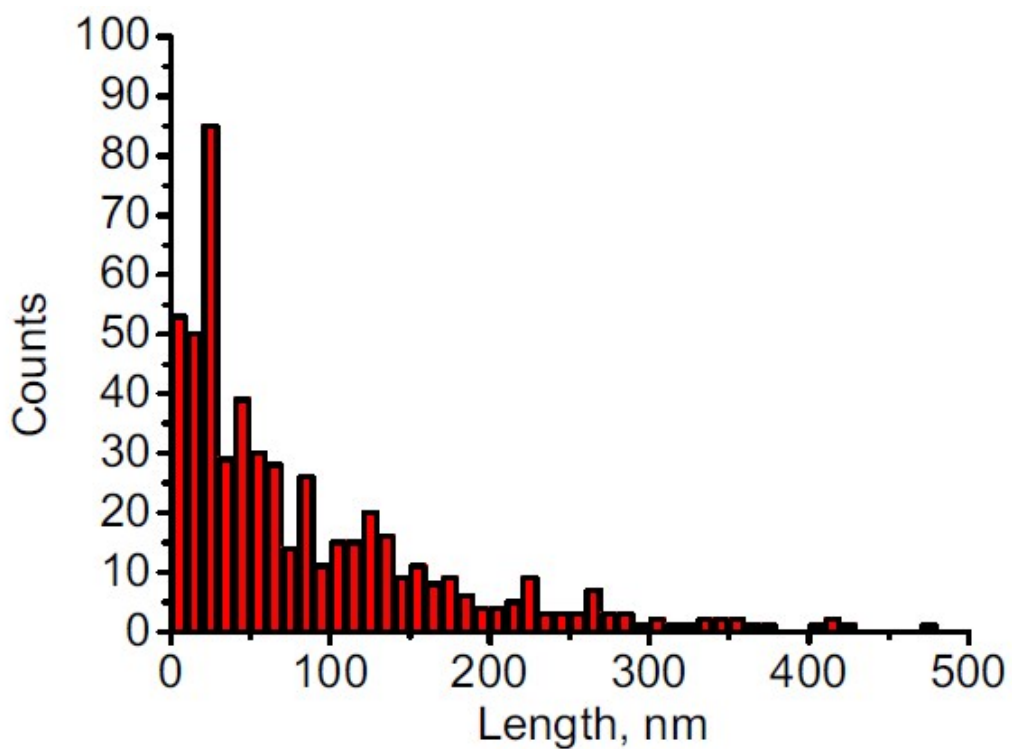
SI Figure 18: AFM image of bet-g-CNCs with $DS = 0.080 \pm 0.003$



SI Figure 19: Size distribution measured with AFM of bet-g-CNCs with $DS = 0.080 \pm 0.003$ with an average size of 104 ± 118 nm.



SI Figure 20: AFM image of bet-g-CNCs with $DS = 0.078 \pm 0.003$



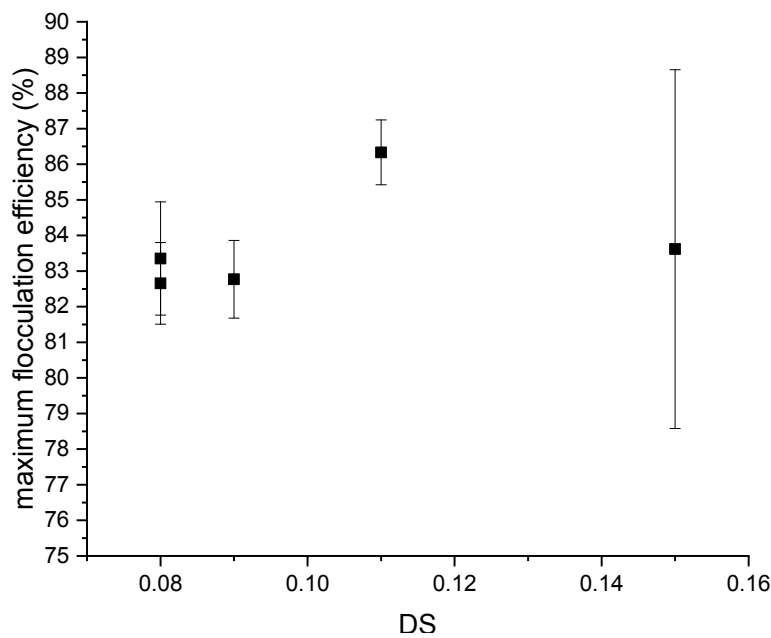
SI Figure 21: Size distribution measured with AFM of bet-g-CNCs with $DS = 0.078 \pm 0.003$ with an average size of 89 ± 100 nm.

S7 Sigmoidal models for dose – response flocculation curves

SI Table 9: P-value, correlation and residual standard error (rse) of the sigmoidal models (dose in mg L⁻¹) of the dose-response curves of all flocculants. The estimated parameters a,b and c as well as there deviation (dev) are shown, and the ratio a/b which

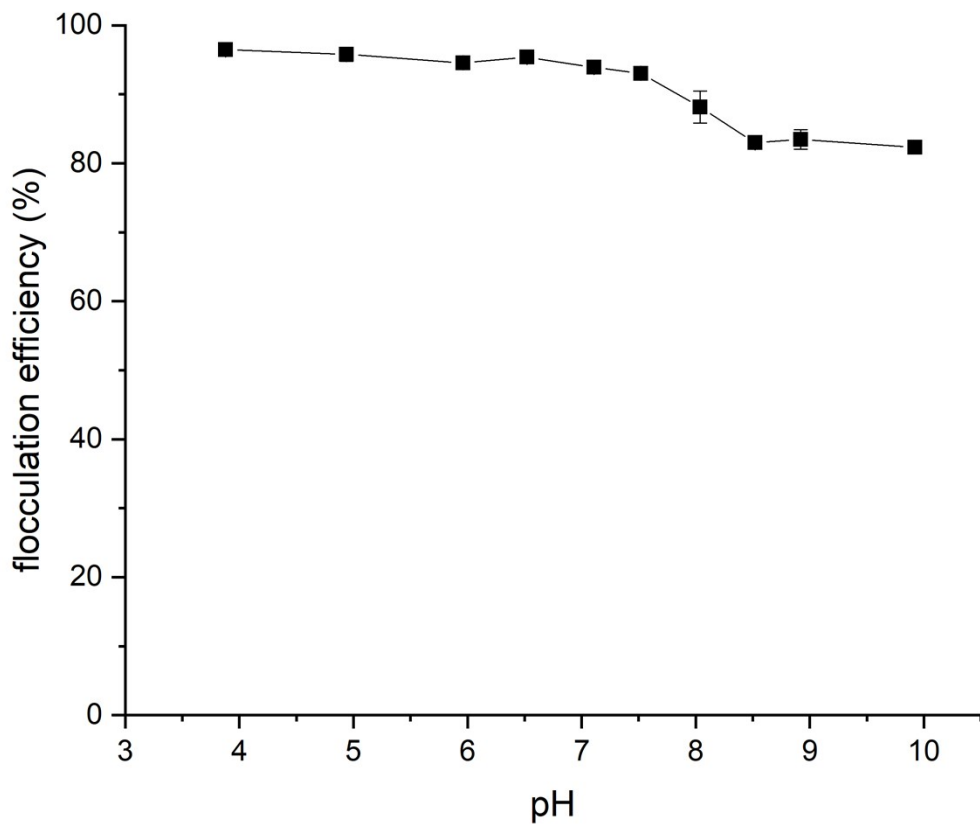
DS	pvalue	correlation	rse	a	deva	b	devb	c	devc	a/b
0.080 ± 0.003	0.171	0.992	4.826	-6.062	1.118	-0.164	0.028	83.352	1.590	37.071
0.078 ± 0.003	0.158	0.996	3.678	-5.468	0.593	-0.172	0.017	82.654	1.145	31.783
0.091 ± 0.004	0.333	0.996	3.643	-7.098	0.967	-0.226	0.028	82.769	1.091	31.345
0.107 ± 0.002	0.098	0.997	3.077	-5.963	0.665	-0.225	0.031	86.334	0.911	26.456
0.152 ± 0.002	0.194	0.880	18.824	-6.152	6.909	-0.317	0.350	83.617	5.039	19.395

equals the inflection point.



SI Figure 22: Degree of substitution of betainium charges onto CNCs vs maximum flocculation efficiency, derived from the sigmoidal models as parameter c.

S8 Flocculation of kaolin at different pH values.



SI Figure 23: Flocculation efficiency of bet-g-CNCs: pH dependance. The used flocculant had a DS = 0.152 ± 0.002 and a dose of 15 mg L⁻¹ was used.